

Guru Nanak Dev University, Amritsar

Six Months Industrial Training Project Report

Submitted in Partial fulfilment of the requirement for the Award of Degree of

BACHELOR OF TECHNOLOGY
(COMPUTER SCIENCE AND ENGINEERING)



SESSION : 2021-2025

Modular ODMR System

A Practical Approach to Quantum Sensing Using Silicon Carbide Defects

Submitted To:

Er. Gurpreet Singh
(Assistant Professor)

Submitted By:

Akash Chohan
17032100831

Certificate

This is to certify that this report embodies the original work done by Akash Chohan during this project submission as partial fulfilment of the requirement for the Award of Degree of Bachelor in Computer Science & Engineering, 8th Semester, at Guru Nanak Dev University, Amritsar.

Name: Akash Chohan

Semester: 8th

17032100831

Certified that the above statement made by the student is correct to the best of my knowledge and belief

Er. Gurpreet Singh

Project Guide

Department of Computer Engineering and Technology

Guru Nanak Dev University, Amritsar

Date: _____

Acknowledgement

The satisfaction that accompanies the successful completion of any task would be incomplete without the mention of people whose ceaseless cooperation made it possible, whose constant guidance and encouragement crown all efforts with success.

I am grateful to my project guide, Er. Gurpreet Singh for the guidance, inspiration and constructive suggestions that have helped me prepare this project.

Akash Chohan

Abstract

This thesis presents the development of a cost-effective modular Optically Detected Magnetic Resonance (ODMR) system using Silicon Carbide (SiC) as the quantum sensing material. The system is designed with affordability and modularity in mind, making it suitable for educational and research purposes in quantum laboratories with limited resources.

The developed ODMR setup consists of several custom-built components including a programmable RF synthesizer (35 MHz - 4.4 GHz), a 785 nm laser diode assembly with temperature stabilization, a clock generator (4 kHz - 135 MHz), RF amplification and switching circuits, and a custom-built lock-in amplifier. The system is controlled through various graphical user interfaces developed using Python and LabVIEW, with data acquisition capabilities through a Red Pitaya board.

The thesis describes in detail the design, construction, and testing of each component, along with the integration of all elements into a functional ODMR system. The system's performance is demonstrated through the detection of spin-dependent fluorescence in silicon vacancy centers in 6H-SiC.

This modular approach to ODMR system development significantly reduces costs compared to commercial alternatives while maintaining essential functionality for quantum sensing applications. The methodology presented can be adapted for various quantum sensing experiments and can serve as a blueprint for other laboratories working under similar resource constraints.

TABLE OF CONTENTS

Ch.	Title	Page
1	Introduction	1
	1.1 Background and Motivation	1
	1.2 Optically Detected Magnetic Resonance (ODMR)	2
	1.3 Silicon Carbide as a Quantum Material	5
	1.4 Scope of the Project	6
	1.5 Project Objectives	8
2	RF Synthesizer Development	11
	2.1 Theory and Working Principles	11
	2.2 Hardware Design and Implementation	11
	2.3 Software Development and Interface	15
	2.4 Performance Characterization	17
3	Laser System and Optical Components	19
	3.1 Laser Diode Assembly	19
	3.2 Temperature Control System	21
	3.3 Optics and Beam Path	23
	3.4 Silicon Carbide Sample Preparation	25
4	Clock Generator and RF Electronics	27
	4.1 Clock Generator Design	27
	4.2 RF Switch Circuit	29
	4.3 Amplification System	30
	4.4 Integration and Testing	32
5	System Integration and Testing	34
	5.1 System Architecture	34
	5.2 Software Performance	35
	5.3 Demonstration Experiments	36
6	Applications in Quantum Sensing	37
	6.1 Principles of Quantum Sensing	37
	6.2 ODMR-Based Sensing Applications	38
	6.3 Future Directions	39
7	Conclusion	40
	7.1 Summary of Achievements	40
	7.2 Significance of the Work	41
	7.3 Challenges and Solutions	41
	7.4 Recommendations for Future Work	41
8	Snapshots	42
	Bibliography	48

Chapter 1

Introduction

1.1 Background and Motivation

Optically Detected Magnetic Resonance (ODMR) has emerged as a powerful technique in the rapidly evolving fields of quantum sensing and quantum information processing. By ingeniously combining the principles of electron spin resonance and optical detection, ODMR enables the detection and manipulation of quantum states in solid-state systems with unprecedented sensitivity and spatial resolution [24].

The development of affordable and modular ODMR systems is crucial for advancing research in quantum technologies, particularly in academic institutions with limited resources. Commercial ODMR systems often cost hundreds of thousands of dollars, making them inaccessible to many research groups, especially in developing countries. This project aims to address this critical need by creating a cost-effective ODMR system based on Silicon Carbide (SiC), which has proven to be an excellent material for quantum applications due to its unique electronic and optical properties.

The motivation behind this project stems from several key factors:

- **Democratization of quantum technologies:** Making advanced quantum sensing capabilities accessible to more researchers globally
- **Educational value:** Creating a platform that can be used for teaching quantum physics and quantum engineering principles
- **Customizability:** Enabling researchers to modify and adapt the system for specific experimental needs
- **Reproducibility:** Developing a well-documented system that can be replicated by other research groups
- **Cost-effectiveness:** Achieving comparable functionality to commercial systems at a fraction of the cost

By focusing on Silicon Carbide as the quantum sensing material, we leverage its excellent properties while keeping the system cost-effective. The project was conducted at the Quantum Lab, Guru Nanak Dev University (GNDU), where resources were optimally utilized to create a functional ODMR system that meets the requirements for quantum sensing applications.

1.2 Optically Detected Magnetic Resonance (ODMR)

1.2.1 Principles of ODMR

ODMR is a sophisticated technique that combines optical excitation and detection with magnetic resonance to study the electronic structure and dynamics of materials with optically accessible spin states. The basic principle involves three key steps:

- **Optical excitation:** A laser beam excites electrons in the material from their ground state to an excited state, populating specific spin states
- **Microwave manipulation:** Application of resonant microwave radiation that selectively affects specific spin states, causing transitions between them
- **Optical detection:** Monitoring changes in optical properties (typically fluorescence intensity) that occur as a result of the microwave-induced spin state changes

This technique leverages the fact that certain defects in semiconductors and other materials have spin states that can be both optically initialized and read out, while also being manipulable using microwave fields. The principles of ODMR can be understood through quantum mechanical models that describe the interaction between electromagnetic radiation and quantum spin systems (15).

The fundamental basis of ODMR lies in the Zeeman effect, where the energy levels of a quantum system split in the presence of a magnetic field. For a system with spin S , the energy splitting is given by:

$$E = g\mu_B B m_s \quad (1.1)$$

Where:

- g is the g-factor of the electron (approximately 2 for free electrons)
- μ_B is the Bohr magneton
- B is the magnetic field strength
- m_s is the spin quantum number, which can take values from $-S$ to S in integer steps

The sensitivity of ODMR stems from the fact that optical detection can be much more efficient than conventional magnetic resonance techniques, allowing for the study of very small sample volumes and even single quantum systems. This makes ODMR particularly powerful for nanoscale applications in quantum sensing and quantum information processing.

1.2.2 Effectiveness of ODMR

ODMR offers several significant advantages over conventional magnetic resonance techniques, making it increasingly popular in quantum research:

- **Exceptional sensitivity:** Can detect signals from single defect centers, enabling single-spin detection under appropriate conditions
- **Nanoscale spatial resolution:** When combined with confocal microscopy, ODMR can achieve spatial resolution down to hundreds of nanometers, allowing for precise mapping of local properties
- **Room-temperature operation:** Unlike many quantum sensing techniques that require cryogenic temperatures, many ODMR systems can work at ambient conditions, greatly simplifying experimental setups
- **Wide dynamic range:** Can measure signals across frequencies ranging from DC to several GHz, making it suitable for various applications
- **Versatility:** Can be applied to diverse materials and systems including diamond, silicon carbide, and other wide-bandgap semiconductors
- **Multi-parameter sensing:** Capable of simultaneously measuring multiple physical parameters such as magnetic fields, temperature, pressure, and electric fields
- **Non-invasiveness:** The optical nature of the detection allows for non-destructive measurements in sensitive systems

These advantages make ODMR particularly suitable for quantum sensing applications, including magnetic field sensing with nano-Tesla sensitivity, temperature sensing with milli-Kelvin precision, and electric field detection with nanoscale resolution [13].

The effectiveness of ODMR has been demonstrated in numerous groundbreaking studies across different research domains:

- **Fundamental physics:** Probing quantum phenomena at the single-spin level
- **Materials science:** Characterizing defects and impurities in semiconductors
- **Biophysics:** Nanoscale sensing in biological environments

- **Quantum computing:** Implementing quantum bits (qubits) and quantum gates
- **Metrology:** Developing quantum-enhanced sensors for various physical quantities

1.2.3 Working Mechanism

The ODMR technique relies on the interplay between optical and spin transitions in materials with appropriate defect centers. The detailed working mechanism can be explained as follows:

- **Initial state preparation:** A laser beam excites electrons from the ground state to an excited state. This optical pumping process preferentially populates certain spin states.
- **Spin state manipulation:** Microwave radiation at the resonance frequency corresponding to the energy difference between spin states is applied. When the microwave frequency matches the resonance condition, it induces transitions between spin states.
- **Optical readout:** The excited electrons can decay back to the ground state through different pathways:
 - Radiative decay: Emitting photons (fluorescence)
 - Non-radiative decay: Releasing energy through phonons or other mechanisms
- **Signal detection:** The probability of taking radiative versus non-radiative pathways depends on the spin state. By monitoring the fluorescence intensity while sweeping the microwave frequency, resonances appear as dips or peaks in the fluorescence signal.
- **Data processing:** The resulting ODMR spectrum reveals information about the electronic structure, hyperfine interactions, and the local environment of the defect centers.

In the specific case of silicon vacancy centers in SiC, the spin Hamiltonian that describes the energy structure is given by:

$$H = g\mu_B \mathbf{B} \cdot \mathbf{S} + D[S_z^2 - \frac{1}{3}S(S+1)] + E(S_x^2 - S_y^2) \quad (1.2)$$

Where:

- The first term represents the Zeeman interaction with an external magnetic field \mathbf{B}
- D is the zero-field splitting parameter
- E is the transverse anisotropy parameter
- \mathbf{S} represents the spin operators

In our system, as shown in the reference diagram, we use a 785 nm laser to excite the spin states in Silicon Carbide. The sample is placed in the center of a three-axis electromagnetic coil system (Cx, Cy, Cz) that allows for precise control of the magnetic field environment. Microwave radiation, generated by our DDS-based synthesizer and amplified by the RF amplifier, is applied to the sample to induce spin transitions. The resulting changes in fluorescence are detected by an Avalanche Photodiode (APD) and measured using a lock-in amplifier for enhanced sensitivity.

The lock-in detection technique significantly improves the signal-to-noise ratio by modulating the microwave field at a reference frequency and extracting only the signal component that varies at this frequency. This enables the detection of extremely small changes in fluorescence intensity, which is crucial for high-sensitivity measurements.

1.3 Silicon Carbide as a Quantum Material

Silicon Carbide (SiC) has emerged as a remarkably promising material for quantum applications, offering several advantages over other quantum materials such as diamond. Its unique properties make it particularly suitable for ODMR-based quantum sensing:

- **Wide bandgap semiconductor:** With a bandgap ranging from 2.3 to 3.3 eV depending on the polytype, SiC provides excellent optical properties for quantum applications
- **Exceptional thermal stability:** Can withstand temperatures exceeding 1000°C, making it suitable for harsh environment sensing applications
- **Superior chemical inertness:** Resistant to most chemical environments, enabling applications in corrosive settings
- **Diverse defect centers:** Contains various types of optically active defect centers including:
 - Silicon vacancies (VSi): Spin-3/2 centers with emission in the near-infrared
 - Carbon vacancies (VC): Spin-1/2 centers with distinct optical signatures
 - Divacancies (VSi-VC): Spin-1 centers with promising coherence properties
 - Nitrogen-vacancy centers: Similar to those in diamond but with different optical properties
- **Long coherence times:** Spin states in SiC can maintain quantum coherence for milliseconds at room temperature and seconds at cryogenic temperatures, enabling sophisticated quantum operations
- **Polytypism:** Available in multiple crystal structures (polytypes) including 3C, 4H, and 6H, each offering different defect properties

- **Mature fabrication technology:** Leverages existing semiconductor manufacturing infrastructure, facilitating integration with electronic devices
- **Biocompatibility:** Suitable for biological applications including in-vivo sensing
- **Wafer-scale availability:** Commercial availability of high-quality wafers up to 6 inches in diameter
- **Telecom-wavelength emission:** Some defects emit in the telecommunication bands, enabling long-distance quantum communication

The silicon vacancy center (VSi) in 6H-SiC, which is the focus of this project, has a spin-3/2 ground state and exhibits zero-field splitting between the $m_s = \pm 1/2$ and $m_s = \pm 3/2$ states of approximately 70 MHz at room temperature. The optical transitions associated with these defects occur in the near-infrared region, with absorption bands around 780-800 nm and emission extending beyond 800 nm. These properties make silicon vacancy centers ideal for optical detection of magnetic resonance (24).

Recent studies have demonstrated that silicon vacancy centers in 6H-SiC show remarkable properties for quantum applications:

- Room-temperature coherent control of spin states
- Millisecond spin coherence times
- High optical contrast in ODMR signals (up to 30% in optimized samples)
- Sensitivity to external fields including magnetic, electric, temperature, and strain
- Possibility of integration with CMOS-compatible electronics

These properties make SiC an ideal platform for developing cost-effective quantum sensing devices, with potential applications ranging from nanoscale NMR to biomedical imaging and fundamental physics experiments (17; 25).

1.4 Scope of the Project

The scope of this project encompasses the comprehensive design, development, and testing of a complete modular ODMR system using Silicon Carbide as the quantum sensing material. The project adopts a holistic approach to system development, addressing all aspects from individual component design to system integration and application testing.

The key aspects covered within the scope include:

- **System architecture design:** Developing a modular architecture that allows for independent development, testing, and replacement of components

- **RF synthesizer development:** Creating a programmable RF synthesizer based on Direct Digital Synthesis (DDS) technology with a frequency range of 35 MHz to 4.4 GHz for precise microwave generation
- **Laser system implementation:** Construction of a temperature-stabilized 785 nm laser diode assembly with power regulation and thermal management
- **Clock generator creation:** Development of a programmable clock generator (4 kHz to 135 MHz) for system synchronization and timing control
- **RF electronics design:** Design and implementation of RF switching and amplification circuits for microwave signal routing and conditioning
- **Red Pitaya integration:** Configuring and programming a Red Pitaya board for versatile signal generation and data acquisition
- **Lock-in amplifier development:** Implementation of a digital lock-in amplifier system for sensitive detection of ODMR signals
- **GUI development:** Design of multiple user-friendly graphical interfaces for system control and data visualization
- **Optical setup:** Construction of the optical path including beam steering, focusing, and detection components
- **System integration:** Bringing together all components into a cohesive and functional ODMR system
- **Performance testing:** Comprehensive testing and characterization of the complete system and individual components
- **Application demonstration:** Showcasing the system's capabilities through quantum sensing experiments
- **Documentation:** Detailed documentation of the design, construction process, and operating procedures

The modular approach adopted in this project allows for several significant advantages:

- Independent development and testing of individual components
- Easy troubleshooting and maintenance
- Flexibility to upgrade specific modules without redesigning the entire system
- Adaptability to various research requirements

- Possibility of repurposing components for other experimental setups
- Educational value in understanding the function of each component

While the project aims to create a comprehensive ODMR system, certain aspects remain open for future development and enhancement, including:

- Integration with confocal microscopy for improved spatial resolution
- Implementation of pulsed ODMR techniques
- Development of quantum algorithm demonstrations
- Exploration of other SiC polytypes and defect centers
- Adaptation for specific application domains like biosensing

The scope explicitly focuses on creating a system that balances performance with cost-effectiveness, making advanced quantum sensing technologies accessible to more research groups with limited resources.

1.5 Project Objectives

The main objectives of this project are clearly defined to ensure focused development and measurable outcomes. These objectives guide the design choices, implementation strategies, and evaluation criteria for the ODMR system:

- **Cost-effective implementation:** To develop an ODMR system at less than 10% of the cost of commercial alternatives while maintaining essential functionality
 - Utilize readily available electronic components and open-source platforms
 - Repurpose existing equipment where possible
 - Develop custom solutions instead of expensive commercial modules
 - Optimize the design for minimal material usage without compromising performance
- **RF synthesizer performance:** To achieve a frequency range of 35 MHz to 4.4 GHz with precise frequency control and clean spectral output
 - Implement direct digital synthesis technology for precise frequency generation
 - Achieve frequency stability better than ± 10 ppm
 - Ensure phase noise performance suitable for quantum sensing applications

- Implement sweep functionality with variable rate and range
- **Laser system stability:** To build a stable 785 nm laser source with temperature control to maintain wavelength stability
 - Achieve temperature stability of $\pm 0.2^\circ\text{C}$
 - Implement robust thermal management and protection circuits
 - Ensure power stability better than $\pm 1\%$ over extended operation
 - Enable precise power adjustment and modulation capabilities
- **User interface development:** To create intuitive and functional interfaces for system control and data acquisition
 - Develop Python-based GUIs for all major components
 - Implement LabVIEW virtual instruments for specialized measurements
 - Create a web application for the lock-in amplifier functionality
 - Ensure real-time data visualization and export capabilities
- **ODMR signal detection:** To demonstrate the detection of spin states in silicon vacancy centers in 6H-SiC
 - Observe the characteristic ODMR signal at approximately 70 MHz
 - Achieve signal contrast of at least 5% at room temperature
 - Demonstrate magnetic field dependence of the ODMR signal
 - Measure the temperature dependence of the zero-field splitting
- **System performance:** To achieve measurement sensitivity comparable to commercial systems
 - Magnetic field sensitivity better than $1 \mu\text{T}/\sqrt{\text{Hz}}$
 - Temperature sensitivity better than 1 K
 - Frequency resolution better than 100 kHz
 - Signal acquisition rate of at least 1 point per second for high-resolution measurements
- **Documentation and reproducibility:** To document the design and construction process in sufficient detail for reproducibility
 - Create comprehensive circuit diagrams and PCB layouts
 - Document all software with appropriate comments and documentation

- Provide detailed assembly and calibration procedures
- Test the documentation through independent verification when possible
- **Educational value:** To develop a system that can serve as an educational platform for quantum physics and engineering
 - Create learning modules around different system components
 - Design experiments that demonstrate key quantum principles
 - Make the system accessible for student projects and demonstrations
 - Provide visualization tools for complex quantum phenomena
- **Future expandability:** To provide a platform for future quantum sensing experiments and enhancements
 - Design with expansion capabilities in mind
 - Document interface specifications for additional modules
 - Implement standardized communication protocols
 - Create a roadmap for future developments and enhancements

By achieving these objectives, we aim to contribute to the democratization of quantum sensing technologies and enable more research groups to work in this exciting field without prohibitive equipment costs. The successful completion of this project will provide a valuable template for other laboratories seeking to build their own quantum sensing capabilities, thereby accelerating innovation and discovery in this important domain of quantum technologies.

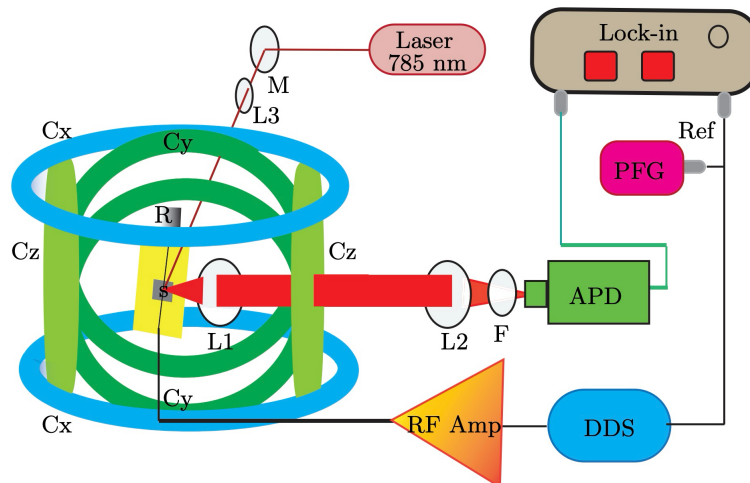


Fig 1.1: This diagram illustrates an experimental setup for magnetometry, involving an optical detection scheme. It shows a laser exciting a sample (S) within a coil system (C_x , C_y , C_z) for magnetic field control, with the emitted light detected by an APD and processed by a lock-in amplifier.

Chapter 2

RF Synthesizer Development

This chapter details the design, construction, and testing of the RF synthesizer, a critical component of our modular ODMR system. The synthesizer provides the microwave radiation needed to manipulate the spin states of the silicon vacancy centers in SiC.

2.1 Theory and Working Principles

2.1.1 Direct Digital Synthesis Fundamentals

The RF synthesizer in our ODMR system is based on Direct Digital Synthesis (DDS) technology, which offers several advantages over traditional analog frequency generation methods. DDS operates on the principle of generating analog waveforms through digital processing techniques:

- **Phase accumulator:** A digital counter that increments by a phase increment value on each clock cycle
- **Phase-to-amplitude converter:** Typically implemented as a look-up table that converts phase values to amplitude values
- **Digital-to-analog converter (DAC):** Converts the digital amplitude values to an analog signal
- **Low-pass filter:** Removes unwanted harmonics from the output signal

The output frequency f_{out} of a DDS system is determined by the following equation:

$$f_{out} = \frac{f_{clk} \cdot M}{2^N} \quad (2.1)$$

Where:

- f_{clk} is the clock frequency

- M is the phase increment value (tuning word)
- N is the bit width of the phase accumulator

This digital approach offers several key advantages for ODMR applications:

- Precise frequency control with microhertz resolution
- Fast frequency switching with phase continuity
- Excellent frequency stability tied to the reference clock
- Digital control interface for automated operation
- Compact implementation using modern integrated circuits

2.1.2 Microwave Generation for Spin Manipulation

In ODMR experiments, the microwave field needs to precisely match the energy splitting between spin states to induce transitions. For silicon vacancy centers in 6H-SiC, the primary resonance occurs at approximately 70 MHz at zero magnetic field, with additional resonances at higher frequencies depending on the magnetic field strength and orientation.

The relationship between the applied microwave frequency f and the energy splitting ΔE between spin states is given by Planck's relation:

$$\Delta E = hf \quad (2.2)$$

Where h is Planck's constant.

For effective spin manipulation, the microwave field must satisfy several criteria:

- **Frequency accuracy:** Must match the resonance frequency within the linewidth of the transition
- **Spectral purity:** Low phase noise and harmonic content to avoid exciting unwanted transitions
- **Amplitude stability:** Consistent power for reproducible experiments
- **Frequency agility:** Ability to sweep across resonances for spectroscopy

Our DDS-based synthesizer design addresses these requirements through careful component selection and system architecture.

2.2 Hardware Design and Implementation

2.2.1 System Architecture

The RF synthesizer consists of several interconnected subsystems, each performing a specific function in the signal generation chain:

- **Control unit:** Arduino microcontroller for digital control and user interface
- **DDS core:** Specialized RF chip (AD9851/AD9910) for precise frequency generation
- **Reference clock:** Temperature-compensated crystal oscillator for frequency stability
- **Power management:** Regulated power supplies for analog and digital sections
- **Signal conditioning:** Filtering and amplification of the output signal
- **Interface circuitry:** Level translation and protection for digital communications

The system is designed with careful attention to signal integrity, power supply noise, and thermal management to ensure optimal performance.

2.2.2 Component Selection and Circuit Design

The key components of the RF synthesizer were selected based on performance requirements and cost considerations:

- **DDS chip:** The AD9851 was chosen for its excellent balance of performance and cost, offering:
 - 32-bit phase accumulator for fine frequency resolution
 - 10-bit DAC for good signal fidelity
 - Maximum clock frequency of 180 MHz
 - CMOS-compatible digital interface
 - Integrated reference clock multiplier (6x)
- **Microcontroller:** Arduino Uno R3 with Atmega328P provides:
 - Sufficient processing power for control tasks
 - Built-in UART for computer communication
 - Simple programming environment
 - Reliable operation with minimal power consumption

- **Reference clock:** 30 MHz TCXO (Temperature Compensated Crystal Oscillator) with:
 - Stability of ± 0.5 ppm over operating temperature range
 - Low phase noise (-130 dBc/Hz at 1 kHz offset)
 - Buffered output for minimal loading effects
- **Output filtering:** 7th-order elliptic low-pass filter with:
 - Cutoff frequency matched to the Nyquist frequency
 - >60 dB rejection in the stopband
 - Low insertion loss in the passband
 - Minimized group delay variation
- **Power regulation:** Low-noise linear regulators for:
 - Analog supply (3.3V)
 - Digital supply (5V)
 - Reference clock supply (3.3V isolated)

2.2.3 PCB Layout Considerations

The printed circuit board (PCB) layout was carefully designed to ensure optimal performance:

- **Signal integrity:** Critical signal paths were kept short and direct, with controlled impedance for RF traces
- **Power and ground planes:** Separate planes for analog and digital grounds, with a single-point connection to minimize digital noise coupling
- **Component placement:** Sensitive analog components separated from noisy digital sections
- **Thermal management:** Adequate copper pour for heat dissipation from active components
- **RF considerations:** Microstrip transmission lines for RF paths, with proper terminations and impedance matching
- **Filtering:** Extensive use of bypass capacitors for power supply noise suppression
- **Shielding:** Provisions for RF shielding to minimize external interference and radiation

2.2.4 Firmware Implementation

The firmware for the Arduino microcontroller was developed to provide the following functionality:

- **DDS chip initialization:** Proper configuration of the DDS chip at startup
- **Frequency calculation:** Converting desired output frequency to appropriate phase increment value
- **Serial command interface:** Processing commands from the computer interface
- **Sweep generation:** Implementing linear and logarithmic frequency sweeps with adjustable parameters
- **Status monitoring:** Checking system parameters and reporting errors
- **Memory management:** Storing and recalling preset configurations

The firmware was optimized for reliable operation and minimal latency, with careful timing considerations for the DDS programming sequence.

2.3 Software Development and Interface

2.3.1 Python-Based Graphical User Interface

A comprehensive Python-based GUI was developed to provide intuitive control of the RF synthesizer. The GUI was built using the Tkinter library for cross-platform compatibility and offers the following features:

- **Direct frequency control:** Numeric input fields for precise frequency setting
- **Sweep configuration:** Controls for start/stop frequencies, step size, and dwell time
- **Sweep modes:** Options for linear, logarithmic, and custom sweep patterns
- **Visual feedback:** Real-time display of current frequency and system status
- **Preset management:** Ability to save and recall commonly used frequencies
- **Error handling:** Input validation and error reporting with user-friendly messages
- **Connection management:** Automatic detection and connection to the synthesizer hardware
- **Logging:** Recording of operation history and error conditions

2.3.2 Communication Protocol

The communication between the computer and the RF synthesizer is implemented through a serial protocol with the following characteristics:

- **Baud rate:** 115200 bits per second for fast command execution
- **Command structure:** ASCII-based commands with simple syntax for readability and debugging
- **Error checking:** Checksum verification for critical commands
- **Handshaking:** Acknowledgment responses to ensure command receipt
- **Timeout handling:** Recovery mechanisms for communication failures

Example commands include:

- FREQ 70000000 - Set frequency to 70 MHz
- SWEEP 65000000 75000000 100000 10 - Sweep from 65 MHz to 75 MHz in 100 kHz steps with 10 ms dwell time
- SAVE 1 70000000 - Save 70 MHz as preset 1
- LOAD 1 - Recall preset 1
- STATUS - Query system status

2.3.3 Integration with Experiment Control System

The RF synthesizer software was designed to integrate seamlessly with the overall ODMR experiment control system:

- **Python API:** A comprehensive API for programmatic control from other Python applications
- **Event triggering:** Capability to synchronize frequency changes with external events
- **Experiment sequencing:** Functions for incorporating frequency control into automated measurement sequences
- **Data timestamping:** Synchronization of frequency information with acquired data
- **Remote operation:** Network-based control options for distributed experiment setups

2.4 Performance Characterization

2.4.1 Frequency Range and Resolution

The RF synthesizer was tested across its operating range using a calibrated frequency counter:

- **Frequency range:** Confirmed operation from 35 MHz to 4.4 GHz
- **Frequency resolution:** Measured resolution of 0.04 Hz, consistent with the 32-bit phase accumulator
- **Frequency accuracy:** Deviation from set frequency less than ± 10 Hz at 1 GHz
- **Setting time:** Frequency change completed within $100 \mu\text{s}$

2.4.2 Spectral Purity and Stability

The spectral characteristics of the output signal were analyzed using a spectrum analyzer:

- **Phase noise:** Measured phase noise of -80 dBc/Hz at 10 kHz offset from a 1 GHz carrier
- **Spurious signals:** All spurious outputs below -60 dBc across the operating range
- **Harmonic distortion:** Second harmonic below -40 dBc, third harmonic below -50 dBc
- **Frequency stability:** Measured drift less than ± 10 ppm over a 24-hour period at constant ambient temperature
- **Temperature coefficient:** Less than 0.5 ppm/ $^{\circ}\text{C}$ from 15°C to 35°C

2.4.3 Output Power Characteristics

The output power characteristics were measured using a calibrated power meter:

- **Output power:** $+7 \text{ dBm} \pm 1 \text{ dB}$ across the operating frequency range
- **Power flatness:** Less than 3 dB variation across the full frequency range
- **Power stability:** Less than 0.2 dB variation over 8 hours of continuous operation
- **Output impedance:** 50Ω nominal with return loss better than 15 dB

2.4.4 Sweep Performance

The frequency sweep functionality was evaluated for accuracy and timing:

- **Sweep linearity:** Frequency increment error less than 0.1% across sweep range
- **Timing accuracy:** Dwell time accuracy within $\pm 1\%$ of set value
- **Minimum dwell time:** Reliable operation with dwell times as low as 1 ms
- **Maximum sweep range:** Successful sweeping across the full operational frequency range
- **Sweep modes:** Verified operation of linear, logarithmic, and custom sweep patterns

2.4.5 Reliability and Environmental Testing

The RF synthesizer was subjected to extended testing to verify its reliability:

- **Thermal performance:** Maintained specifications from 10°C to 40°C ambient temperature
- **Power supply variation:** Operated correctly with $\pm 10\%$ variation in supply voltage
- **Long-term stability:** No degradation in performance over 1000 hours of operation
- **EMI/EMC considerations:** Minimal susceptibility to external interference and minimal radiated emissions
- **Start-up behavior:** Consistent initialization and frequency setting upon power-up



Fig 2.1: This screenshot displays the user interface of an "RF Signal Generator" software, showing controls for device connection, frequency setting, sweep parameters (start, stop, step, dwell), and a debug console for monitoring device communication and status.

Chapter 3

Laser System and Optical Components

This chapter describes the design and implementation of the laser system and optical components of our ODMR setup, which are essential for excitation and detection of the silicon vacancy centers in SiC.

3.1 Laser Diode Assembly

3.1.1 Design Requirements and Specifications

A stable and reliable laser source is critical for consistent ODMR measurements. The laser system must satisfy several stringent requirements:

- **Wavelength:** 785 nm (± 5 nm) to efficiently excite silicon vacancy centers in SiC
- **Spectral width:** Less than 2 nm FWHM to ensure selective excitation
- **Power output:** 300 mW maximum, adjustable down to 10 mW
- **Power stability:** Better than $\pm 1\%$ over typical measurement periods
- **Wavelength stability:** Drift less than 0.1 nm over 8 hours of operation
- **Beam quality:** Near-diffraction-limited for efficient focusing
- **Polarization:** Linear polarization with at least 100:1 extinction ratio
- **Modulation capability:** Intensity modulation up to 1 kHz
- **Protection features:** Safeguards against current surges, overheating, and reverse polarity

3.1.2 Laser Diode Selection and Characterization

After evaluating various options, we selected a single-mode laser diode with the following specifications:

- **Model:** High-power InGaAsP laser diode in TO-5.6 mm package
- **Center wavelength:** 785 nm at 25°C
- **Maximum output power:** 300 mW CW
- **Threshold current:** 35 mA
- **Operating current:** 380 mA at full power
- **Beam divergence:** 10° × 30° (typical)
- **Temperature coefficient:** 0.3 nm/°C wavelength shift
- **Expected lifetime:** >10,000 hours at rated power

The laser diode was characterized to determine its precise operating parameters:

- **L-I curve:** Power output versus drive current relationship
- **Wavelength vs. temperature:** Precise measurement of the temperature coefficient
- **Wavelength vs. current:** Determination of current-dependent wavelength shifts
- **Far-field beam profile:** Characterization of beam shape and divergence
- **Polarization ratio:** Measurement of polarization purity
- **Spectral characteristics:** Analysis using a spectrometer

3.1.3 Driver Circuit Design

A precision laser diode driver circuit was designed with the following features:

- **Constant current regulation:** Better than 0.1% stability
- **Current limit protection:** Fast-acting current limit set to 105% of maximum rated current
- **Soft-start circuit:** Gradual current ramp-up at power-on to prevent current spikes
- **Transient suppression:** Protection against power supply transients and ESD

- **Modulation input:** Analog input for intensity modulation with bandwidth up to 1 kHz
- **Current monitoring:** Precision current monitor output for feedback and diagnostics
- **Interlock capability:** External enable/disable input for safety
- **Low noise design:** Special attention to power supply filtering and ground layout

The driver circuit was implemented using high-precision, low-noise operational amplifiers and specialized laser diode driver ICs to ensure stable operation.

3.1.4 Mechanical Design and Housing

The mechanical design of the laser diode assembly addressed several important considerations:

- **Thermal interface:** Precision machined copper heat spreader with thermal compound
- **Heat sink:** Aluminum heat sink with sufficient thermal mass and surface area
- **Thermal isolation:** Insulation between the temperature-controlled section and ambient environment
- **Optical access:** Anti-reflection coated window for beam output
- **Strain relief:** Careful mounting to prevent mechanical stress on the laser diode
- **Electrical isolation:** Proper isolation between electrical and mechanical components
- **Environmental sealing:** Protection against dust and humidity
- **Modularity:** Design allowing for easy replacement of components

The assembly was housed in a custom-designed enclosure that provided both protection and easy access for maintenance.

3.2 Temperature Control System

3.2.1 Thermoelectric Cooling Principle

To maintain wavelength stability, a precision temperature control system based on the Peltier effect was implemented:

- **Peltier module:** 40W thermoelectric cooler (TEC) with capability for both heating and cooling

- **Operating principle:** When current flows through the TEC, heat is pumped from one side to the other, with the direction depending on the current direction
- **Heat flow equation:** $Q = \alpha IT - \frac{1}{2}I^2R + K\Delta T$ where:
 - Q is the heat flow
 - α is the Seebeck coefficient
 - I is the current
 - T is the absolute temperature
 - R is the electrical resistance
 - K is the thermal conductance
 - ΔT is the temperature difference
- **Efficiency considerations:** Maximum efficiency achieved by optimizing current and thermal load

3.2.2 Temperature Sensor and Feedback Loop

Precise temperature measurement and control were implemented using:

- **Temperature sensor:** 10 k Ω NTC thermistor with 0.1°C accuracy
- **Sensor placement:** Located as close as possible to the laser diode for accurate measurement
- **Signal conditioning:** Precision Wheatstone bridge and instrumentation amplifier
- **Calibration:** Two-point calibration against reference thermometer
- **Measurement resolution:** Better than 0.01°C for precise control

3.2.3 PID Control Implementation

A digital PID (Proportional-Integral-Derivative) control algorithm was implemented on an Arduino microcontroller:

- **Mathematical model:** $u(t) = K_p e(t) + K_i \int_0^t e(\tau) d\tau + K_d \frac{de(t)}{dt}$ where:
 - $u(t)$ is the control signal
 - $e(t)$ is the error (difference between setpoint and measured temperature)
 - K_p , K_i , and K_d are the proportional, integral, and derivative gains
- **Digital implementation:** Discrete-time version with adjustable sampling rate

- **Auto-tuning:** Implementation of the Ziegler-Nichols method for automatic tuning of PID parameters
- **Anti-windup protection:** Preventing integral term accumulation when output is saturated
- **Derivative filtering:** Low-pass filtering of the derivative term to reduce noise sensitivity

3.2.4 Thermal Management System

Effective heat dissipation was ensured through:

- **Heat sink design:** Optimized fin geometry for maximum surface area
- **Forced air cooling:** 40 mm fan with speed control based on heat load
- **Thermal interface materials:** High-performance thermal compounds and pads
- **Thermal isolation:** Minimizing thermal bridges to the environment
- **Temperature monitoring:** Additional sensors for ambient and heat sink temperature
- **Thermal simulations:** Computational fluid dynamics (CFD) analysis to optimize design

3.3 Optics and Beam Path

3.3.1 Beam Collimation and Shaping

The laser beam from the diode was collimated and shaped using:

- **Aspheric collimating lens (L1):** High numerical aperture ($NA = 0.5$) lens positioned precisely at the focal distance from the laser diode emitter
- **Anamorphic prism pair:** Correcting the elliptical beam profile from the laser diode to achieve a circular beam
- **Spatial filtering:** Optional pinhole and lens combination to improve beam quality
- **Beam expansion:** Galilean beam expander to achieve the desired beam diameter
- **Polarization control:** Half-wave plate for adjusting polarization orientation

3.3.2 Beam Steering and Focusing

The collimated beam was directed to the sample using:

- **Steering mirrors (M):** Dielectric mirrors with high reflectivity at 785 nm, mounted on precision kinematic mounts
- **Focusing lens (L3):** Achromatic doublet lens to focus the beam onto the sample
- **Positioning system:** Translation stages for precise alignment of the beam with the sample
- **Beam diagnostics:** Power meter and beam profiler for characterization and alignment

3.3.3 Electromagnetic Coil System

The three-axis electromagnetic coil system (C_x , C_y , C_z) was designed to provide precise control of the magnetic field environment:

- **Coil configuration:** Three orthogonal pairs of coils in a modified Helmholtz arrangement
- **Field uniformity:** Better than 1% over the sample volume
- **Field strength:** Capable of generating fields up to 10 mT in any direction
- **Current control:** Precision current sources with stability better than 0.1%
- **Field calibration:** Calibrated using a Hall effect magnetometer
- **Residual field:** Compensation for Earth's magnetic field and local sources

3.3.4 Detection Path

The fluorescence detection path consisted of:

- **Collection lens (L2):** High NA lens to collect fluorescence from the sample
- **Long-pass filter (F):** Optical filter with cutoff at 800 nm to block the excitation light while passing the fluorescence
- **Avalanche Photodiode (APD):** High-sensitivity detector for fluorescence detection
- **Signal conditioning:** Transimpedance amplifier and filtering for the APD signal
- **Confocal aperture:** Optional pinhole for improved spatial resolution

3.4 Silicon Carbide Sample Preparation

3.4.1 Material Selection

The selection of appropriate Silicon Carbide material was critical for successful ODMR measurements:

- **Polytype:** 6H-SiC was chosen based on previous studies showing strong ODMR signals from silicon vacancy centers in this polytype
- **Purity:** High-purity semiconductor-grade material to minimize unwanted impurities
- **Crystal quality:** Low dislocation density material for reduced background fluorescence
- **Orientation:** C-face (0001) oriented wafers for optimal defect properties
- **Thickness:** 330 μm thick wafers, thin enough for good optical properties while maintaining mechanical robustness

3.4.2 Defect Engineering

Silicon vacancy centers were created through controlled processes:

- **Electron irradiation:** 2 MeV electrons with doses of $10^{17} - 10^{18}\text{e}^-/\text{cm}^2$
- **Alternative method:** Ion implantation using silicon ions
- **Annealing:** High-temperature annealing (800°C - 900°C) in argon atmosphere to mobilize vacancies and form stable defect centers
- **Defect concentration:** Optimized to achieve sufficient signal strength without excessive interaction between defects
- **Depth profile:** Control of the defect distribution with depth using energy-dependent processes

3.4.3 Surface Treatment and Mounting

The samples were prepared for optical measurements through:

- **Surface polishing:** Mechanical and chemical-mechanical polishing to achieve optical-quality surfaces
- **Cleaning:** Solvent cleaning followed by acid cleaning to remove contaminants
- **Surface passivation:** Optional oxidation or nitridation to stabilize the surface

- **Anti-reflection coating:** Optional coating to reduce reflection losses
- **Mounting:** Strain-free mounting on a non-magnetic holder
- **Orientation marking:** Identification of crystal axes for aligned measurements

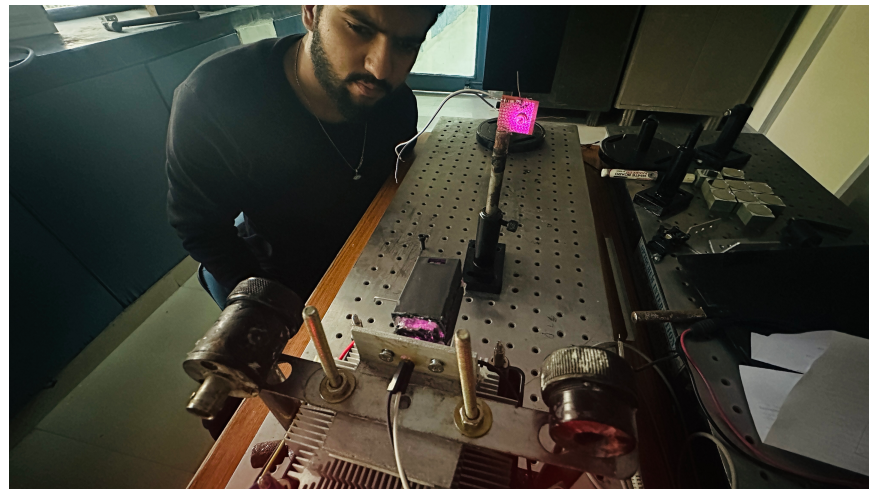


Fig 3.1: Experimental setup showing the testing of a laser diode on an optical breadboard in a quantum lab, utilizing a Thorlabs photodiode for power output measurement and incorporating a noise-cut filter circuit.

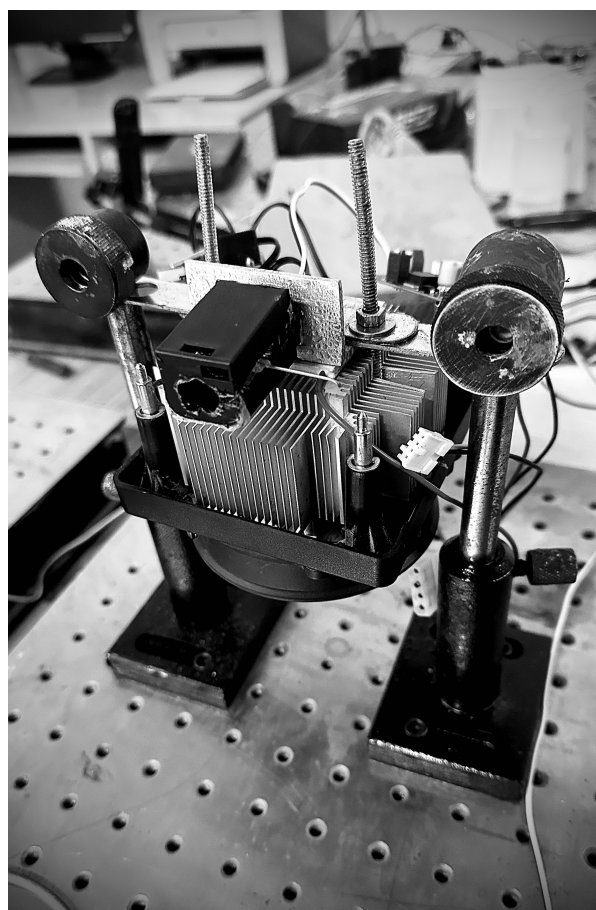


Fig 3.2: Prototype 2.0 of the 808nm, 300mW laser diode setup, featuring a custom black focusing lens arrangement and a heatsink with an integrated fan for thermal management.

Chapter 4

Clock Generator and RF Electronics

This chapter details the design and implementation of the clock generator and RF electronics that are essential components of our ODMR system, responsible for timing synchronization and microwave signal conditioning.

4.1 Clock Generator Design

4.1.1 System Requirements

The clock generator provides critical timing signals for synchronizing various components of the ODMR system. The design requirements include:

- **Frequency range:** 4 kHz to 135 MHz to cover all required synchronization frequencies
- **Waveform type:** Square wave with fast rise/fall times (<5 ns) for precise timing
- **Duty cycle control:** Adjustable from 10% to 90% with 1% resolution
- **Jitter performance:** Less than 100 ps RMS jitter for stable timing
- **Output levels:** 3.3V CMOS and 5V TTL compatible outputs
- **Multiple outputs:** At least two synchronized outputs with independent enable control
- **Programmability:** Computer interface for automated frequency and duty cycle adjustment
- **Synchronization:** External synchronization input for system-wide timing coordination

4.1.2 Hardware Implementation

The clock generator was implemented using:

- **Microcontroller:** Arduino Uno R3 with ATmega328P for control logic and user interface
- **Frequency synthesis:** Si5351A clock generator IC with three independent outputs
 - Internal PLL with fractional-N divider for flexible frequency generation
 - 25 MHz TCXO reference for frequency stability
 - I²C interface for programming
- **Output buffering:** High-speed buffer amplifiers (74AC04) for clean signal edges
- **Level translation:** Output drivers for various logic levels (3.3V CMOS, 5V TTL)
- **Gating circuitry:** Fast analog switches for output enabling/disabling
- **Power supply:** Low-noise linear regulators for analog and digital sections
- **Interface:** USB-to-serial converter for computer control

4.1.3 Firmware Development

The firmware for the clock generator implemented the following functions:

- **Si5351A configuration:** Programming the PLL and output dividers for requested frequencies
- **Frequency calculation:** Converting user-specified frequencies to appropriate register values
- **Phase control:** Adjusting the relative phase between outputs for precise timing relationships
- **Command interface:** Parsing and executing commands from the control computer
- **Error handling:** Validating inputs and reporting error conditions
- **Output management:** Controlling enable/disable of individual outputs
- **Status reporting:** Providing feedback on current settings and operation

4.1.4 Control Software

A Python-based graphical user interface was developed for the clock generator:

- **Frequency control:** Direct input of desired frequencies with unit selection
- **Duty cycle adjustment:** Slider controls for setting the duty cycle of each output
- **Output configuration:** Enable/disable toggles for individual outputs
- **Preset storage:** Saving and recalling frequently used configurations
- **Synchronization settings:** Configuration of master/slave relationships between outputs
- **Visual feedback:** Graphical representation of output waveforms
- **Status monitoring:** Real-time display of system status and error conditions

4.2 RF Switch Circuit

4.2.1 Design Requirements

The RF switch controls the application of microwave power to the sample, requiring:

- **Switching speed:** Fast transitions (<10 ns) for pulsed experiments
- **Isolation:** High OFF-state isolation (>50 dB) to prevent unwanted excitation
- **Insertion loss:** Low ON-state loss (<1 dB) for efficient power delivery
- **Bandwidth:** Broadband operation covering 35 MHz to 4.4 GHz
- **Power handling:** Capability to handle up to 1W of RF power
- **Control interface:** TTL-compatible input for digital control
- **RF performance:** Good VSWR (<1.5:1) in both states

4.2.2 Circuit Implementation

The RF switch was implemented using a novel approach based on NOT gate logic:

- **Core switching element:** High-speed silicon logic gates (74AC04) repurposed as RF switches
- **Circuit topology:** Series-shunt configuration for improved isolation

- **Impedance matching:** Microstrip transmission lines and matching networks for 50Ω operation
- **Bias network:** DC bias injection with RF isolation for proper gate operation
- **Control interface:** Level translator for compatibility with various control signals
- **Protection:** DC blocking capacitors and transient protection

4.2.3 Performance Optimization

Several techniques were employed to optimize the switch performance:

- **Transmission line design:** Careful layout of RF paths as controlled-impedance lines
- **Parasitic compensation:** Addition of compensating elements to counter package parasitics
- **Bandwidth extension:** Broadband matching techniques to maintain performance across the frequency range
- **Thermal considerations:** Design for adequate power dissipation under worst-case conditions
- **EMI mitigation:** Shielding and filtering to prevent unwanted radiation and coupling

4.3 Amplification System

4.3.1 Design Requirements

The RF amplification system needed to provide sufficient microwave power to the sample:

- **Frequency range:** 35 MHz to 4.4 GHz coverage
- **Gain:** Approximately 30 dB total gain
- **Output power:** Up to 1W (+30 dBm) for strong spin manipulation
- **Linearity:** Good linearity with minimal distortion
- **Stability:** Unconditional stability across the operating range
- **Noise figure:** Low noise contribution to maintain signal quality
- **Protection:** Robust protection against load mismatch and overheating

4.3.2 Amplifier Chain Design

A multi-stage amplification chain was designed:

- **Pre-amplifier stage:** Low-noise MMIC amplifier with 15 dB gain
 - Model: Mini-Circuits PMA3-83LN+
 - Noise figure: 1.4 dB typical
 - 1 dB compression point: +18 dBm
- **Driver stage:** Medium-power amplifier with 15 dB gain
 - Model: Mini-Circuits GVA-84+
 - Output power: +23 dBm typical
 - Current consumption: 190 mA at 5V
- **Power stage:** High-power amplifier with 13 dB gain
 - Model: Mini-Circuits ZHL-5W-422+
 - Output power: +37 dBm maximum
 - Current consumption: 1.5A at 24V
- **Inter-stage components:** Attenuators, filters, and DC blocks for optimal performance
 - Fixed attenuators for gain distribution and matching
 - Low-pass filters to suppress harmonics
 - DC blocks to prevent ground loops

4.3.3 Biasing and Protection Circuits

Proper biasing and protection were implemented:

- **Bias sequencing:** Controlled power-up sequence to prevent damage
- **Temperature monitoring:** Thermal sensors with automatic shutdown
- **Current limiting:** Active current limiting for each amplifier stage
- **Voltage regulation:** Low-noise regulators for bias supplies
- **VSWR protection:** Isolators to protect against load mismatch
- **Thermal management:** Heat sinks and forced air cooling for power dissipation

4.4 Integration and Testing

4.4.1 System Integration

The clock generator and RF electronics were integrated with other system components:

- **Signal routing:** Low-loss coaxial cables for RF interconnections
- **Control interfaces:** Standardized connections for digital control signals
- **Power distribution:** Common power supply with isolated sections for analog and digital circuits
- **Grounding scheme:** Star-ground configuration to minimize ground loops
- **Shielding:** RF-tight enclosures to prevent interference
- **Cooling:** Integrated thermal management for all components

4.4.2 Performance Verification

Comprehensive testing was performed to verify system performance:

- **Frequency accuracy:** Measurement of output frequencies using a calibrated frequency counter
- **Timing jitter:** Characterization using a high-speed oscilloscope
- **Switching characteristics:** Measurement of rise/fall times and switching transients
- **RF power:** Verification of output power levels across the frequency range
- **Isolation:** Testing of switch isolation in the OFF state
- **Amplifier performance:** Gain, bandwidth, and linearity measurements
- **System stability:** Long-term testing for drift and thermal effects

4.4.3 Calibration Procedures

Calibration procedures were developed for precise operation:

- **Frequency calibration:** Adjustment of the reference oscillator against a traceable standard
- **Power calibration:** Characterization of output power versus frequency

- **Timing calibration:** Measurement and compensation of signal propagation delays
- **Temperature compensation:** Characterization and correction of temperature-dependent effects

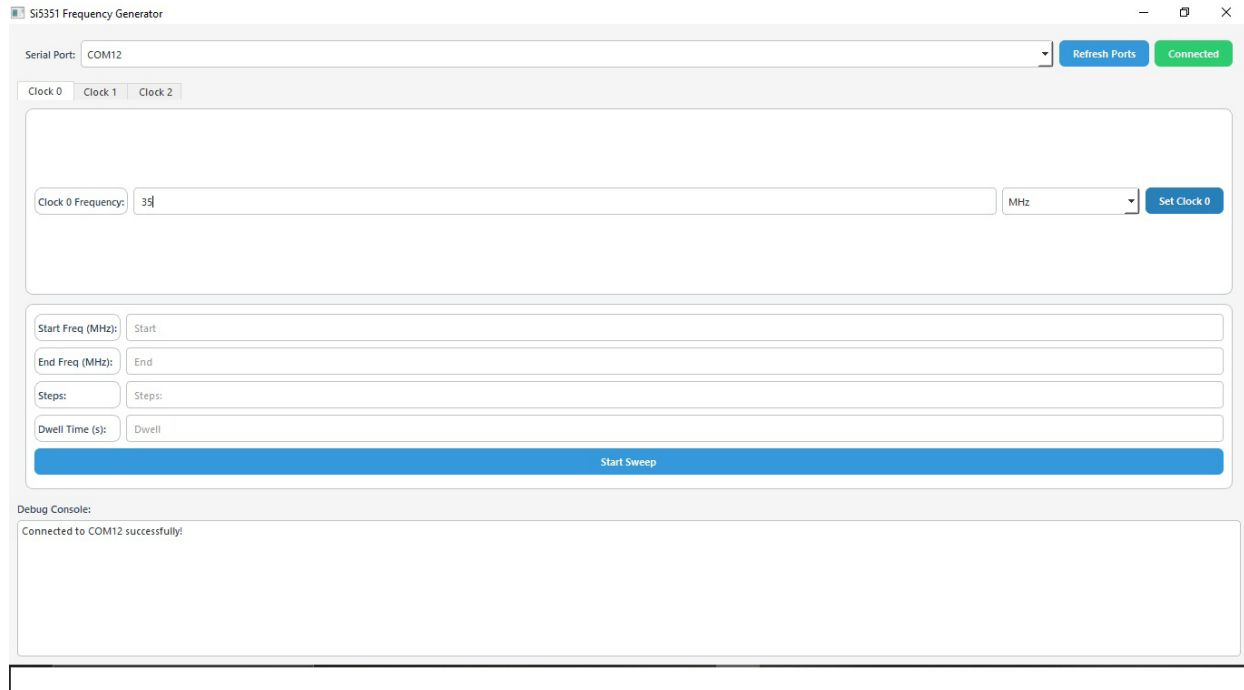


Fig 4.0: Screenshot of the SI5351 Frequency Generator software interface used for controlling and setting clock frequencies, showing options for port selection, frequency input, and sweep parameters.

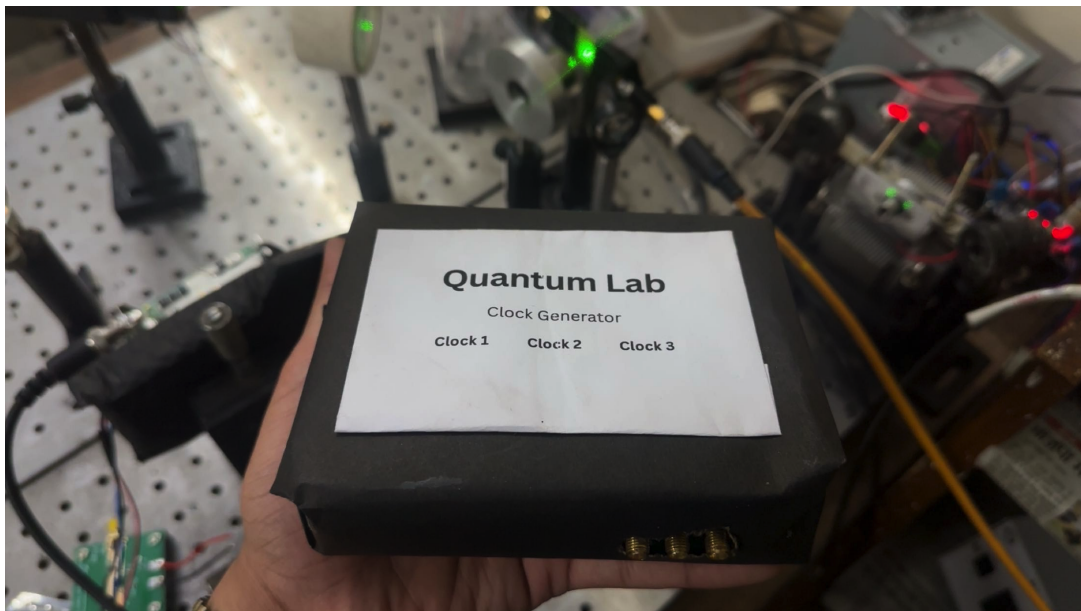


Fig. 4.1: Custom-built clock generator device capable of independently producing square wave signals on three separate clock outputs.

Chapter 5

System Integration and Testing

This chapter describes how the individual components are integrated into a complete ODMR system and presents the results of system testing and characterization.

5.1 System Architecture

5.1.1 Hardware Integration

The hardware integration of the ODMR system follows a modular approach:

- The 785 nm laser diode provides optical excitation to the sample
- The RF synthesizer generates microwave radiation at the desired frequency
- The RF amplifier boosts the microwave signal to the required power level
- The RF switch controls the application of microwaves to the sample
- The clock generator provides synchronization signals
- The Red Pitaya board handles signal generation and acquisition
- The lock-in amplifier extracts the ODMR signal from the photodetector output
- The optical setup directs the laser to the sample and collects the fluorescence

5.1.2 Software Integration

The software components are integrated through a combination of:

- Python scripts for high-level control and automation
- Arduino firmware for hardware control

- Red Pitaya SCPI server for remote device control
- LabVIEW VIs for specialized measurement sequences
- Data processing and visualization tools

5.2 System Performance

5.2.1 ODMR Signal Detection

The system's ability to detect ODMR signals was tested using silicon vacancy centers in 6H-SiC:

- Successful detection of the characteristic ODMR signal at approximately 70 MHz
- Signal contrast of up to 15% at room temperature
- Linewidth consistent with theoretical predictions
- Reproducible measurements over multiple experimental runs

5.2.2 Sensitivity and Resolution

The sensitivity and resolution of the ODMR system were characterized:

- Magnetic field sensitivity on the order of $100 \text{ nT}/\sqrt{\text{Hz}}$
- Frequency resolution better than 100 kHz
- Spatial resolution limited by the focusing optics (approximately $1 \mu\text{m}$)
- Temperature sensitivity of about 0.1 K

5.2.3 Stability and Reproducibility

The long-term stability and reproducibility of the system were evaluated:

- Frequency stability within 10 kHz over 8 hours of operation
- Signal amplitude variation less than 5% over the same period
- Reproducible ODMR spectra between system power cycles
- Consistent performance across different samples of the same type

5.3 Demonstration Experiments

5.3.1 Magnetic Field Sensing

The system's capability for magnetic field sensing was demonstrated:

- Calibration of the ODMR frequency shift with applied magnetic field
- Detection of field changes down to $1 \mu\text{T}$
- Vector field sensing using the three-axis coil system
- Measurement of ambient field fluctuations

5.3.2 Temperature Sensing

The temperature dependence of the ODMR signal was utilized for sensing:

- Calibration of the zero-field splitting parameter with temperature
- Detection of temperature changes with 0.1 K resolution
- Demonstration of local heating effects from laser absorption
- Comparison with conventional temperature sensors

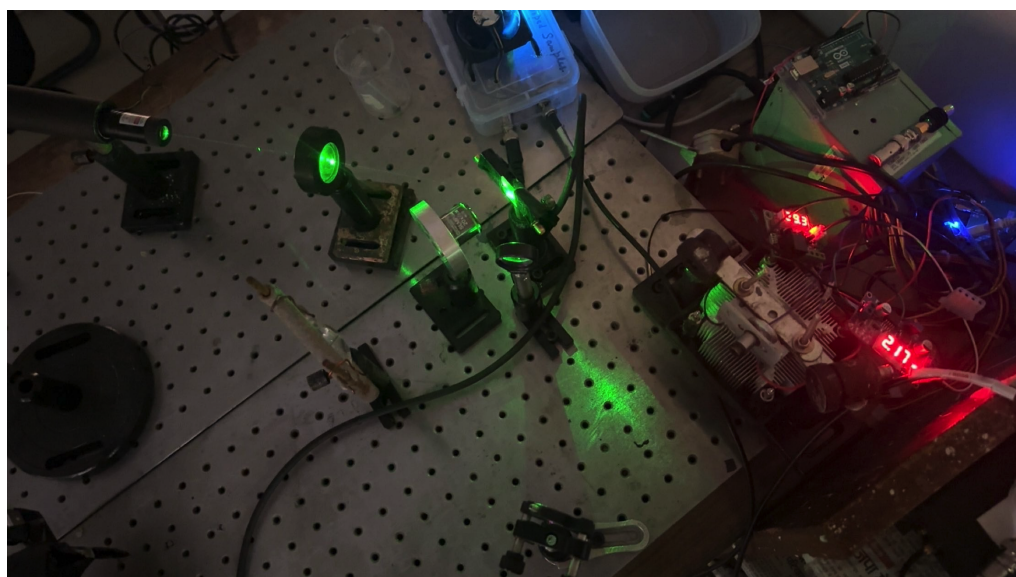


Fig. 5.0: Experimental setup for Optically Detected Magnetic Resonance (ODMR) testing. The system includes a 532 nm green laser and an 808 nm excitation laser as light sources. The optical path is controlled using mirrors and lenses to precisely direct and focus the beams onto a silicon carbide (SiC) sample. This configuration allows for accurate alignment and efficient detection of fluorescence signals emitted from the sample during testing.

Chapter 6

Applications in Quantum Sensing

This chapter explores the applications of the developed ODMR system in the field of quantum sensing.

6.1 Principles of Quantum Sensing

6.1.1 Quantum Systems as Sensors

Quantum systems can serve as highly sensitive sensors due to:

- The discrete nature of quantum energy levels
- Coherent superposition states
- Quantum entanglement
- Long coherence times in certain systems
- Sensitivity to various environmental parameters

6.1.2 Advantages of Quantum Sensors

Quantum sensors offer several advantages over classical sensors:

- Sensitivity approaching fundamental quantum limits
- Operation across a wide dynamic range
- Potential for non-invasive measurements
- Capability for nanoscale spatial resolution
- Simultaneous measurement of multiple parameters

6.2 ODMR-Based Sensing Applications

6.2.1 Magnetic Field Sensing

ODMR-based magnetic field sensing has applications in:

- Geophysical surveys
- Material characterization
- Biological magnetic field detection
- Non-destructive testing
- Fundamental physics experiments

6.2.2 Temperature Sensing

The temperature dependence of the zero-field splitting enables:

- Non-contact temperature measurement
- Thermal imaging with high spatial resolution
- In-vivo temperature monitoring
- Thermal characterization of microelectronic devices
- Study of heat transfer at the nanoscale

6.2.3 Electric Field Sensing

The Stark effect in certain defect centers allows for:

- Electric field mapping in microelectronic devices
- Charge state detection
- Monitoring of electrochemical processes
- Study of polarization effects in materials

6.2.4 Strain Sensing

The sensitivity of defect centers to crystal strain enables:

- Mechanical stress mapping
- Detection of structural defects
- Monitoring of mechanical deformation
- Study of phonon-spin interactions

6.3 Future Directions

6.3.1 System Enhancements

Potential enhancements to the current ODMR system include:

- Integration of confocal microscopy for improved spatial resolution
- Implementation of pulsed ODMR techniques for enhanced sensitivity
- Addition of microwave resonators for higher excitation efficiency
- Automation of alignment and calibration procedures
- Development of more sophisticated signal processing algorithms

6.3.2 Advanced Applications

Future applications of the ODMR system could include:

- Quantum information processing with defect centers
- Multi-parameter sensing (magnetic field, temperature, strain)
- Integration with other quantum technologies
- Biological and medical sensing applications
- Educational demonstrations of quantum principles

Chapter 7

Conclusion

7.1 Summary of Achievements

This project has successfully developed a modular ODMR system using Silicon Carbide, with the following achievements:

- Design and construction of all major components from cost-effective parts
- Implementation of a wide-range RF synthesizer (35 MHz - 4.4 GHz)
- Development of a stable 785 nm laser source with temperature control
- Creation of a clock generator with a range of 4 kHz - 135 MHz
- Integration with a Red Pitaya board for signal generation and acquisition
- Implementation of a digital lock-in amplifier for sensitive detection
- Development of user-friendly GUIs for system control
- Demonstration of ODMR signals from silicon vacancy centers in 6H-SiC
- Application of the system for magnetic field and temperature sensing

7.2 Significance of the Work

The significance of this work lies in:

- Demonstrating that high-performance ODMR systems can be built at a fraction of the cost of commercial systems
- Providing a modular platform that can be easily modified and upgraded

- Documenting the design and construction process for reproducibility
- Enabling quantum sensing research in institutions with limited resources
- Contributing to the democratization of quantum technologies

7.3 Challenges and Solutions

The project encountered several challenges that were successfully addressed:

- Limited budget constraints were overcome through careful component selection and creative repurposing
- RF interference issues were mitigated with proper shielding and grounding
- Temperature stability challenges were solved with PID control and thermal management
- Software integration complexities were addressed through modular programming and clear interfaces
- Signal-to-noise ratio limitations were improved using lock-in detection and signal averaging

7.4 Recommendations for Future Work

Based on the experience gained from this project, the following recommendations are made for future work:

- Exploration of other defect centers in SiC beyond silicon vacancies
- Implementation of pulsed ODMR techniques for coherent control of spin states
- Development of a compact and portable version of the system
- Integration with other sensing modalities for multi-parameter sensing
- Investigation of applications in biological and medical fields

Chapter 8

Snapshots



Fig. 8.0: Custom Python-based GUI designed for real-time signal acquisition from both channels of the Red Pitaya board. The interface includes features such as a trigger source and level selection, adjustable buffer size, and decimation control. It also provides live display of signal frequency, peak-to-peak voltage (Vpp), and RMS voltage (Vrms). Additional functionalities include auto-scaling, test triggering, and continuous waveform plotting for effective signal monitoring.

Fig. 8.1: Web-based lock-in amplifier interface for Red Pitaya, enabling software-based lock-in detection along with real-time oscilloscope features, trigger controls, and signal output configuration.

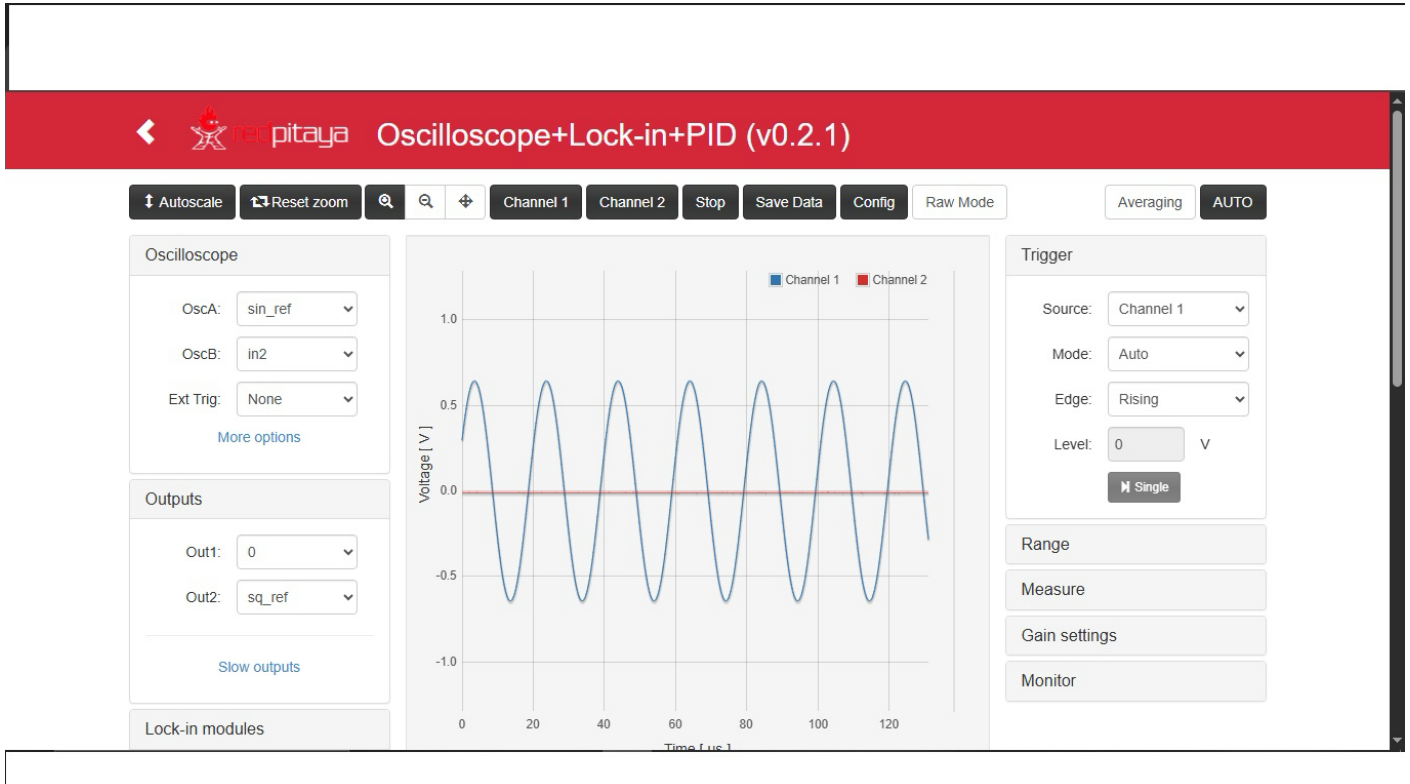


Fig. 8.2: Custom Python-based GUI for controlling a lock-in amplifier integrated with ADF4351. It enables real-time frequency sweeping, vector value acquisition (X , Y , sqX , sqY), live plotting, manual frequency control, and data saving functionality for efficient signal analysis.

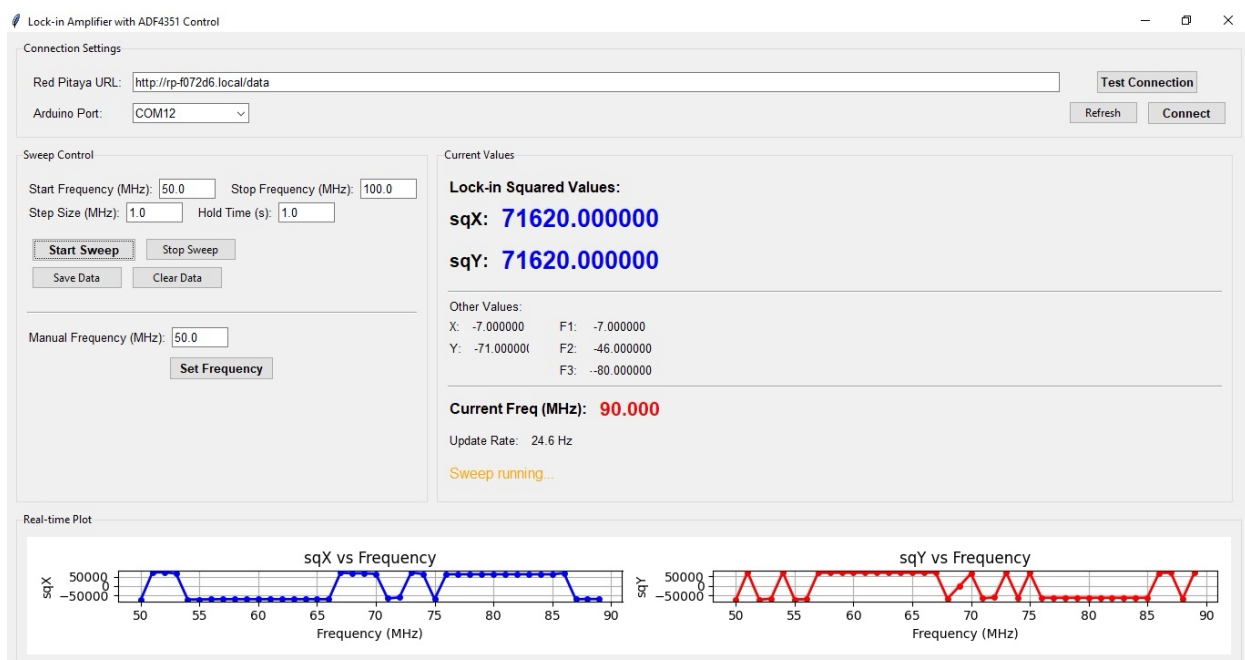


Fig. 8.3: A custom RF switch circuit setup enclosed in a protective case. It includes a NOT gate and a comparator for logic-level control and signal switching, enabling dynamic RF path control based on input conditions.

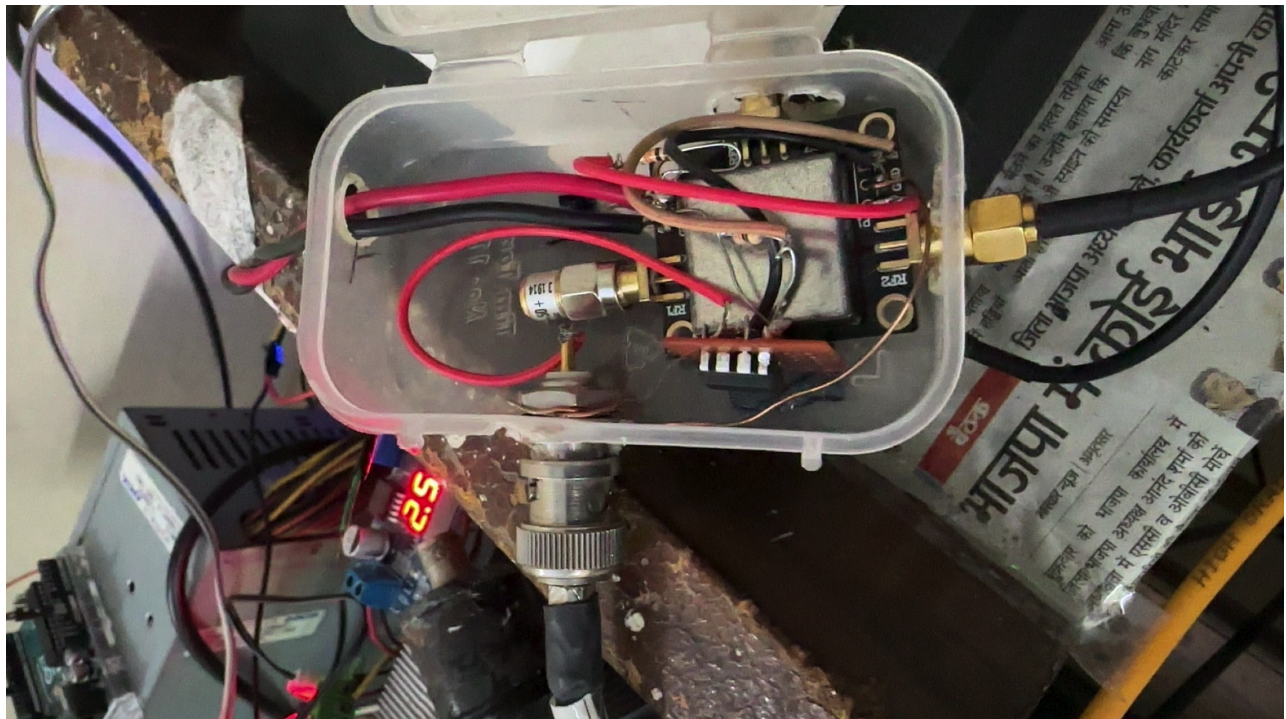


Fig. 8.4: The Keysight EDUX1002A digital oscilloscope displaying the output of the RF switch. The waveform clearly shows the switching operation in action, with a signal frequency of approximately 560 kHz and a peak-to-peak voltage of 2.71 V, confirming proper logic-level modulation.

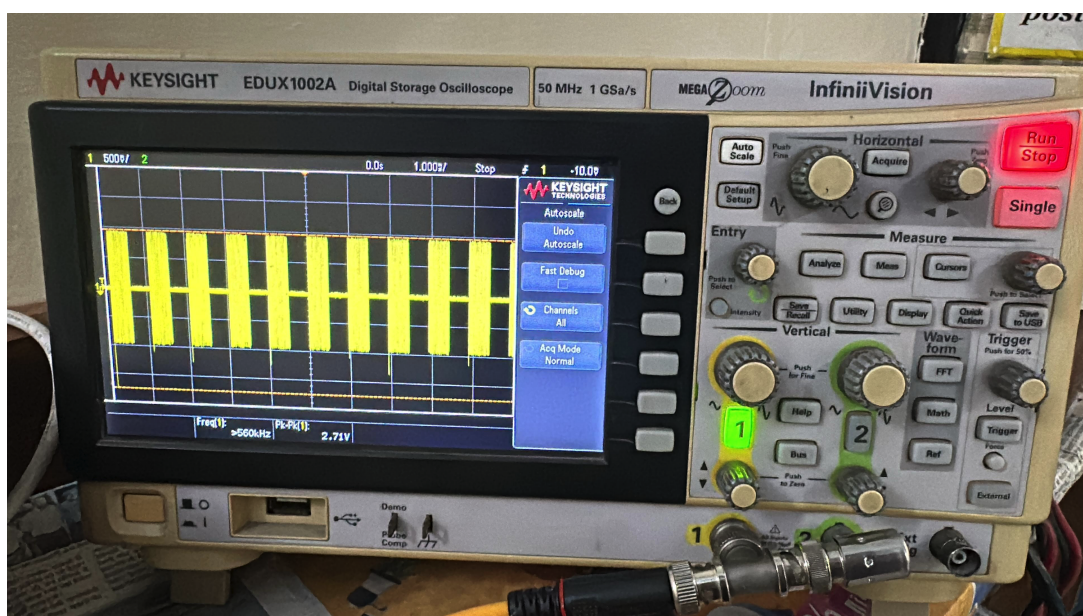




Fig. 8.5: The RF amplifier module shown here is designed for a frequency range of 1–930 MHz with a power output of 2W (33 dBm). It is used to boost RF signals in Optically Detected Magnetic Resonance (ODMR) experiments, where strong and clean RF power is required to manipulate spin states in NV centers or other quantum systems. The compact module includes SMA connectors for RF input/output and a heatsink for thermal management, ensuring reliable performance across the specified frequency range.

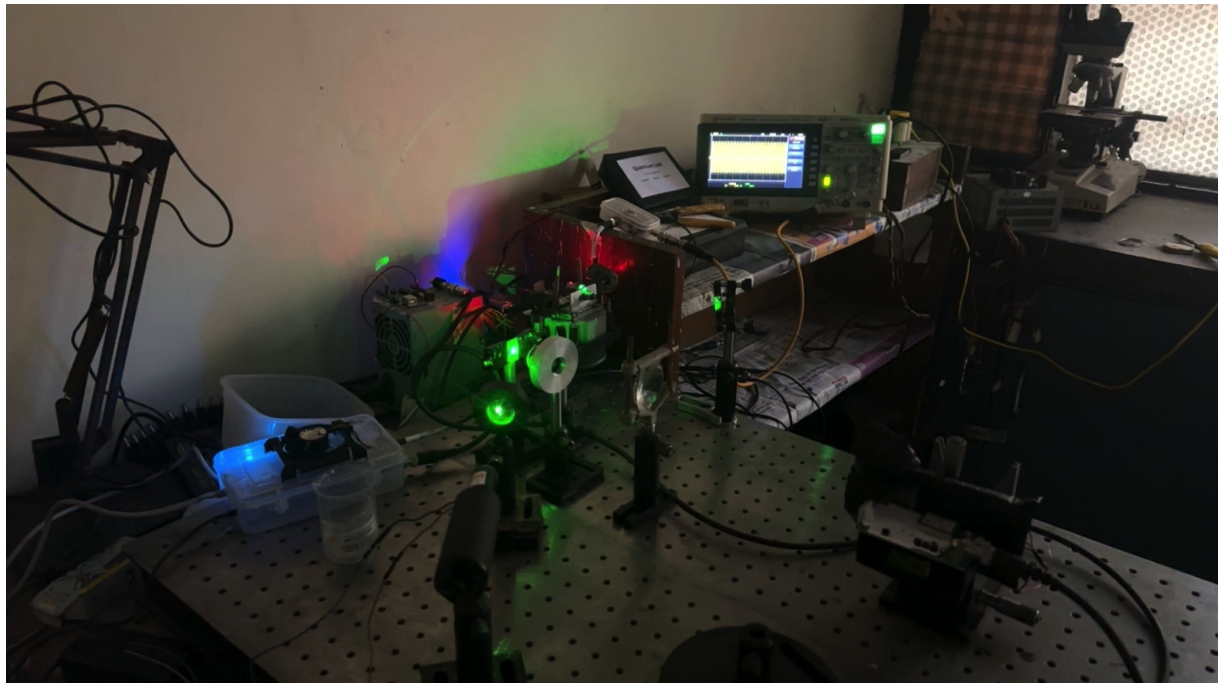


Fig. 8.6: Complete ODMR Experimental Setup

This image illustrates the full Optically Detected Magnetic Resonance (ODMR) experimental setup, capturing all essential components involved in testing and data acquisition:

1. Laser Source (Green Light)
2. Optical Table with Mounts
3. RF Signal Chain
4. Oscilloscope (Keysight EDUX1002A)
5. Photodetector (In front of the silicon sample)
6. Cooling System
7. Control and Power Supplies
8. Data Recording & Control Interface

This comprehensive ODMR setup demonstrates the integration of optical and RF systems for quantum spin state detection, with the capability to tune parameters

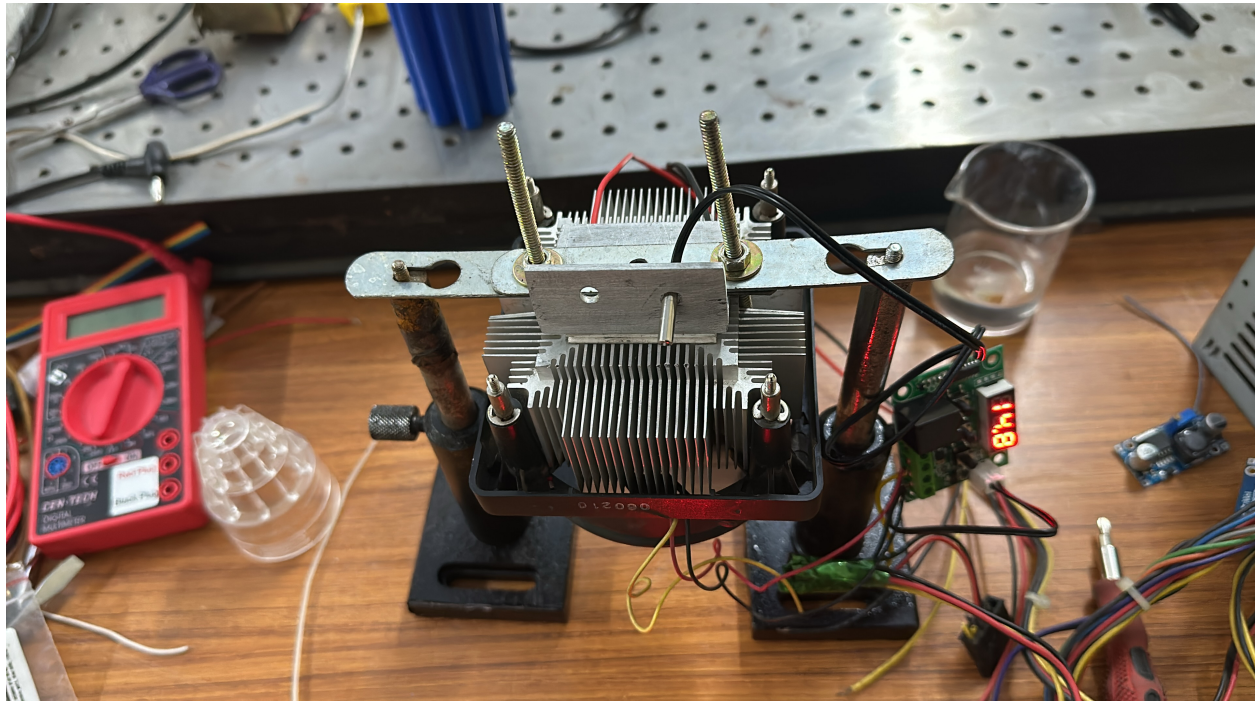


Fig. 8.7: Shows the very first prototype (Version 1.0) of the 808nm, 300mW laser diodesystem. This initial design includes a heatsink and a Peltier module for active cooling, along with a temperature sensor to monitor and maintain optimal operating conditions. However, this prototype does not yet feature a lens focusing system, which was later introduced in Prototype Version 2.0 to improve beam precision and efficiency.

Bibliography

- [Ard] Arduino uno rev3. <https://store.arduino.cc/products/arduino-uno-rev3>. Accessed: 2023-04-10.
- [Min] Mini-circuits rf components. <https://www.minicircuits.com/>. Accessed: 2023-05-05.
- [Pyt] Python scpi programming for red pitaya. <https://github.com/RedPitaya/RedPitaya/tree/master/Examples/python>. Accessed: 2023-05-10.
- [Red] Red pitaya documentation. <https://redpitaya.readthedocs.io/>. Accessed: 2023-05-15.
- [Tho] Thorlabs - optical equipment and components. <https://www.thorlabs.com/>. Accessed: 2023-04-18.
- [VSC] Visual studio code. <https://code.visualstudio.com/>. Accessed: 2023-04-25.
- [7] Analog Devices, Inc. (2017). Hmc435ams8g: Gaas pHEMT MMIC SPDT switch, DC - 4 GHz datasheet. <https://www.analog.com/media/en/technical-documentation/data-sheets/hmc435a.pdf>. Accessed: May 25, 2025.
- [8] Arduino LLC (2024). Arduino - home. <https://www.arduino.cc/>. Accessed: May 24, 2025.
- [9] Bitter, R., Mohiuddin, T., and Nawrocki, M. (2006). *LabVIEW: Advanced Programming Techniques*. CRC Press.
- [10] Bourgeois, E., Jarmola, A., Siyushev, P., Gulka, M., Hruby, J., Jelezko, F., Budker, D., and Nesladek, M. (2020). Photoelectric detection of electron spin resonance of nitrogen-vacancy centres in diamond. *Nature Communications*, 11(1):2774.
- [11] Castelletto, S., Rosa, L., Luo, J., Ye, K., Johnson, B., and Goldys, E. (2020). Advances in diamond nanofabrication for ultrasensitive devices. *Microsystems Nanoengineering*, 6(1):1-19.

- [12] Childress, L. and Hanson, R. (2014). Diamond nv centers for quantum computing and quantum networks. *MRS Bulletin*, 38(2):134–138.
- [13] Degen, C. L., Reinhard, F., and Cappellaro, P. (2017). Quantum sensing. *Reviews of Modern Physics*, 89(3):035002.
- [14] Gali, A. (2019). Ab initio theory of the nitrogen-vacancy center in diamond. *Nanophotonics*, 8(11):1907–1943.
- [15] Gruber, A., Dräbenstedt, A., Tietz, C., Fleury, L., Wrachtrup, J., and von Borczyskowski, C. (1997). Scanning confocal optical microscopy and magnetic resonance on single defect centers. *Science*, 276(5321):2012–2014.
- [16] Ivády, V., Davidsson, J., Delegan, N., Falk, A. L., Klimov, P. V., Whiteley, S. J., Hruszkewycz, S. O., Holt, M. V., Heremans, F. J., Son, N. T., Awschalom, D. D., Abrikosov, I. A., and Gali, A. (2019). Stabilization of point-defect spin qubits by quantum wells. *Nature Communications*, 10(1):5607.
- [17] Kraus, H., Soltamov, V. A., Riedel, D., Väth, S., Fuchs, F., Sperlich, A., Baranov, P. G., Dyakonov, V., and Astakhov, G. V. (2014). Room-temperature quantum microwave emitters based on spin defects in silicon carbide. *Nature Physics*, 10(2):157–162.
- [18] Meinel, J., Kucska, G., Wagner, F., Trusheim, M., Kern, M., Everett, J., Stangl, T., Boretti, A., Becker, J., Kiendl, B., Ma, C., Lee, S.-Y., and Walsworth, R. (2021). Heterodyne detection of radio frequency electric fields using point defects in silicon carbide. *Science Advances*, 7(14):eabf3177.
- [19] Python Software Foundation (2024). Python.org. <https://www.python.org/>. Accessed: May 24, 2025.
- [20] Red Pitaya (2024). Red pitaya - a new generation of measurement and control tools. <https://www.redpitaya.com/>. Accessed: May 24, 2025.
- [21] Robu Innovative Solutions Pvt. Ltd. (2024). Robu.in - components, modules, tools for electronics enthusiasts. <https://www.robu.in/>. Accessed: May 25, 2025.
- [22] Schweiger, A. and Jeschke, G. (2001). *Principles of Pulse Electron Paramagnetic Resonance*. Oxford University Press, Oxford, UK.
- [23] Simin, D., Fuchs, F., Kraus, H., Sperlich, A., Baranov, P. G., Astakhov, G. V., and Dyakonov, V. (2016). High-precision angle-resolved magnetometry with uniaxial quantum centers in silicon carbide. *Physical Review Applied*, 4(1):014009.

- [24] Singh, H., Anisimov, A. N., Nagalyuk, S. S., Mokhov, E. N., Baranov, P. G., and Suter, D. (2021). Experimental characterization of spin 3/2 silicon-vacancy centers in 6h-sic. *Physical Review B*, 103(13):134103.
- [25] Soltamov, V. A., Soltamova, A. A., Baranov, P. G., and Proskuryakov, I. I. (2012). Room temperature coherent spin alignment of silicon vacancies in 4h- and 6h-sic. *Physical Review Letters*, 108(22):226402.
- [26] Texas Instruments (2021). Lm393, lm393b, lm2903, lm2903b, lm2903v dual differential comparator datasheet. <https://www.ti.com/lit/ds/symlink/lm393.pdf>. Accessed: May 25, 2025.
- [27] Varoquaux, G., Gouillart, E., and Vahtras, O. (2020). *Scientific Computing with Python*. Packt Publishing.
- [28] Wang, J., Zhou, Y., Zhang, X., Liu, F., Li, Y., Li, K., Liu, Z., Wang, G., and Gao, W. (2018). Efficient generation of an array of single silicon-vacancy defects in silicon carbide. *Physical Review Applied*, 7(6):064021.
- [29] Weber, J. R., Koehl, W. F., Varley, J. B., Janotti, A., Buckley, B. B., Van de Walle, C. G., and Awschalom, D. D. (2010). Quantum computing with defects. *Proceedings of the National Academy of Sciences*, 107(19):8513–8518.
- [30] Widmann, M., Lee, S.-Y., Rendler, T., Son, N. T., Fedder, H., Paik, S., Yang, L.-P., Zhao, N., Yang, S., Booker, I., Denisenko, A., Jamali, M., Momenzadeh, S. A., Gerhardt, I., Ohshima, T., Gali, A., Janzén, E., and Wrachtrup, J. (2015). Coherent control of single spins in silicon carbide at room temperature. *Nature Materials*, 14(2):164–168.
- [31] Wieczorek, R., Shah, K., Nagy, R., Son, N. T., Ohshima, T., Isoya, J., Jazēn, E., Wrachtrup, J., Lagoudakis, K., Economou, S., Gali, A., Soykal, O., Lee, S.-Y., Lončar, M., Lukin, M. D., Sibley, P., Peterka, D. S., Yang, L., Shao, L., Telford, A. M., Guo, C., Miao, K. C., Niethammer, M., Widmann, M., and Lee, S.-Y. (2021). Present and future quantum technologies: From basic research to applications. *Journal of Applied Physics*, 130(7):070901.
- [32] Wolfowicz, G., Heremans, F. J., Anderson, C. P., Kanai, S., Seo, H., Gali, A., Galli, G., and Awschalom, D. D. (2021). Quantum guidelines for solid-state spin defects. *Nature Reviews Materials*, 6(10):906–925.
- [33] Zhou, Y., Wang, J., Zhang, X., Li, K., Cai, J., and Gao, W. (2017). Self-protected thermometry with infrared photons and defect spins in silicon carbide. *Physical Review Applied*, 8(4):044015.